Phenomenological models for the gap anisotropy of $Bi_2Sr_2CaCu_2O_8$ as measured by angle-resolved photoemission spectroscopy

M. R. Norman and M. Randeria
Materials Science Division, Argonne National Laboratory, Argonne, Illinois 60439

H. Ding and J. C. Campuzano
Materials Science Division, Argonne National Laboratory, Argonne, Illinois 60439
and Department of Physics, University of Illinois at Chicago, Chicago, Illinois 60607
(Received 13 December 1994)

Recently, high resolution angle-resolved photoemission spectroscopy has been used to determine the detailed momentum dependence of the superconducting gap in the high-temperature superconductor $Bi_2Sr_2CaCu_2O_8$. In this paper, we first describe tight-binding fits to the normal-state dispersion and superlattice modulation effects. We then discuss various theoretical models in light of the gap measurements. We find that the simplest model which fits the data is the anisotropic s-wave gap $\cos(k_x)\cos(k_y)$, which within a one-band BCS framework suggests the importance of next-near-neighbor Cu-Cu interactions. Various alternative interpretations of the observed gap are also discussed, along with the implications for microscopic theories of high-temperature superconductors.

I. INTRODUCTION

One of the key issues today in the field of high-temperature superconductivity is the symmetry of the superconducting order parameter. Penetration depth measurements[1] on Y-Ba-Cu-O indicate that the gap has line nodes in momentum space. This information by itself is not sufficient to determine the symmetry of the order parameter. Various Josephson interference experiments[2,3] on Y-Ba-Cu-O are consistent with an order parameter which has $d_{x^2-y^2}$ symmetry; some of these directly probe the sign change in the the order parameter under a 90° rotation.[2] These results are, however, not consistent with c-axis Josephson tunneling data[4] and other interference experiments.[5] The situation is made even more confusing by experiments on other high-T_c materials: penetration depth measurements[6] and tunneling data[7] on Nd-Ce-Cu-O and tunneling data on the single layer Hg cuprate[8] indicate an apparently isotropic gap.

The improvement in resolution of angle-resolved photoemission spectroscopy (ARPES) as well as the large gaps associated with the high transition temperatures of the cuprates allows the possibility of directly mapping out the momentum dependence of the gap. We are indeed fortunate that the (quasi) two-dimensional nature of the cuprates allows ARPES to directly measure the spectral function of the electrons. Recently, the Stanford group[9] presented the first ARPES data indicating significant momentum anisotropy in the gap function for the two layer Bi cuprate (Bi-2212), with the gap being large along the CuO bond direction $(\pi,0)$ and small, possibly zero, in the diagonal direction (π,π) in contrast to early ARPES data[10] on Bi-2212 which showed no gap anisotropy. More recent work[11,12] has confirmed the Stanford results and found that the observed gap anisotropy is sensitive to sample quality and surface conditions[11] with some samples showing a much smaller, though nonzero,[12] gap along the (π,π) direction compared with that along $(\pi,0)$. Even in the Stanford data the anisotropy decreased significantly with sample aging, probably due to gas absorption on the surface.[9] It must be mentioned that attempts to see the gap with ARPES on other cuprates, particularly Y-Ba-Cu-O have not been successful. The reason appears to be that in Bi-2212 the cleavage is between the two BiO layers which are van der Waals coupled. Thus, the act of cleavage minimally disrupts the sample surface, as opposed to YBCO where chain copper − apical oxygen bonds are broken.[13]

Recently, our group has measured the detailed momentum dependence of the gap in Bi-2212 on very high-quality samples[14] employing a spectrometer with improved energy resolution (described by a Gaussian of standard deviation 8 meV).[15] These results are consistent with the earlier work discussed above, but with improved resolution, were able to demonstrate that the nodes in the gap function were not along the (π,π) directions as one would have for a gap of $d_{x^2-y^2}$ symmetry, but rather displaced at an angle of 10° to both sides of the diagonal direction. The purpose of this paper is to discuss the detailed angle dependence of the gap, and see which theoretical models are consistent with such a gap function.

Our main results are summarized below.

(1) We give a tight-binding fit to the normal-state dispersion data which reproduces the experimentally observed Fermi surface.

(2) We note that there is no clear evidence for two CuO bands, suggesting that the bilayer splitting is either weak

0163-1829/95/52(1)/615(8)/$06.00

or nonexistent.

(3) The occupied area of the Fermi surface corresponds to a hole doping of 17%.

(4) We demonstrate that data in the Y quadrant are consistent with the superlattice modulation observed in structural studies.

(5) The observed momentum dependence of the superconducting gap is not compatible with pure $d_{x^2-y^2}$ pairing. We also argue that the data are not consistent with a dirty d-wave or a mixed ($s+d$, $s+id$, or $d+g$) gap.

(6) The observed gap in the X quadrant is consistent with an interplay between a pure $d_{x^2-y^2}$ state and the superlattice modulation. However this interpretation is not consistent with the data in the Y quadrant.

(7) A mixed $s \pm d$ gap coming from pairing within a bilayer can fit the data but at the expense of having two gaps at each k point. So far there is no evidence in our data for such a two-gap spectrum.

(8) The simplest interpretation of the data is in terms of anisotropic s-wave pairing. An s_{xy} gap function with $\Delta(\mathbf{k}) = \Delta_0 \cos(k_x)\cos(k_y)$ provides an excellent fit to the data.

(9) s_{xy} pairing would arise within a BCS framework from next-near-neighbor (Cu-Cu) attraction with weak on-site repulsion.

(10) Several microscopic theories which lead to anisotropic s-wave pairing are discussed in relation to the data, including models based on charge transfer, extended saddle points, and interlayer tunneling.

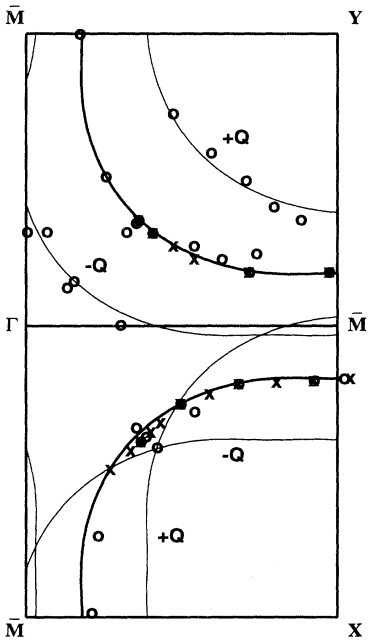

FIG. 1. Fermi surface points measured by ARPES. Open circles were measurements in the normal state, crosses in the superconducting state. The thick line represents a tight-binding fit to the data as described in the text. The thin lines are displaced from this by the superlattice Q vector, and are marked by $+Q$ and $-Q$.

TABLE I. Tight-binding basis functions used in fitting the experimental energy dispersions as described in the text. In this notation, the Y point is (π,π). The first column lists the coefficient of each term (eV), that is $\epsilon(\vec{k}) = \sum c_i \eta_i(\vec{k})$.

c_i	$\eta_i(\vec{k})$
0.1305	1
-0.5951	$\frac{1}{2}(\cos k_x + \cos k_y)$
0.1636	$\cos k_x \cos k_y$
-0.0519	$\frac{1}{2}(\cos 2k_x + \cos 2k_y)$
-0.1117	$\frac{1}{2}(\cos 2k_x \cos k_y + \cos k_x \cos 2k_y)$
0.0510	$\cos 2k_x \cos 2k_y$

II. NORMAL STATE

We use the notation $\bar{M} = (\pi,0)$, $X = (\pi,-\pi)$, $Y = (\pi,\pi)$, and $\Gamma = (0,0)$ where $\Gamma - \bar{M}$ is along the CuO bond direction and (x,y) refers to the square lattice reciprocal cell. X and Y are slightly inequivalent since the average unit cell in Bi-2212 is orthorhombic, with axes $\sqrt{2}$ times the square lattice axes and rotated 45° relative to them (the a and b axes differ by only 0.1%). The X and Y quadrants, though, do differ strongly because of the presence of an incommensurate superlattice in the BiO planes directed along one of the orthorhombic axes with a corresponding wave vector, Q along $\Gamma - Y$ of $(0.21\pi, 0.21\pi)$.[16]

We turn now to the normal-state data. The circles and crosses in Fig. 1 are the Fermi surface crossings in the ARPES measurements in the normal and superconducting states, respectively, and the thick line is the Fermi surface of the tight-binding fit described below. We used six tight-binding functions to fit the normal-state dispersion data (the latter determined by the peak positions of the ARPES spectra), with the functions and their coefficients listed in Table I. The six conditions used to determine the coefficients were (1) two points from the measured energy dispersion in the ΓY direction, (2) two points from the measured dispersion in the $\Gamma\bar{M}$ direction, (3) the measured Fermi surface crossing in the $\bar{M}Y$ direction, and (4) the energy at the Y point. The latter is not experimentally determined (since it corresponds to an unoccupied state) but is a necessary constraint to obtain a good fit. The criteria used was to note that the energy dispersion below the Fermi energy looks like that of band theory,[17] just reduced by a factor of 2, as previously noted by Olson's group.[18] Therefore, we assumed the same (i.e., half the band theory value) to be true above the Fermi energy to obtain the energy at the Y point. The resulting energy dispersion fit is shown in Fig. 2. This looks similar to that inferred by the Stanford group[19] with two differences. First, the energy of the $\bar{M}$ point is definitely below the Fermi energy (−34 meV), and, second, only one CuO band is seen, not the two that might have been expected due to the two CuO planes/unit cell. These differences are primarily due to the increased energy resolution of the present experiments.

This indicates that the bilayer splitting is either very

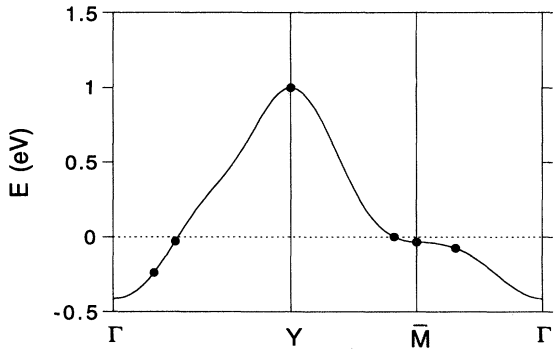

FIG. 2. Energy dispersion from the tight-binding fit. The filled circles were data points used in the fit (the Y point being obtained as described in the text). Note the extended van Hove singularity at the $\bar{M}$ point.

weak or nonexistent. Although this is consistent with band theory results at the Fermi energy, band theory in addition predicts a sizable splitting at the $\bar{M}$ point related to interactions with BiO bands. Such a splitting and the existence of BiO bands below the Fermi energy does not appear to be consistent with our data. Absence of bilayer splitting, though, is consistent with theories based on incoherent c-axis transport.[20] We contrast this with Y-Ba-Cu-O, where significant bilayer splitting has been seen in ARPES measurements[21] (consistent with band theory). This difference is due to the presence of chains in Y-Ba-Cu-O which couple differently to the even and odd combinations of the bilayer, which together with the buckling of the CuO layers, causes a sizable splitting.[22]

We also note from Fig. 1 the presence of side sheets in the Y quadrant. The Q vector connecting the side sheets to the main sheet is within our resolution equal to the superlattice Q vector, $0.21(\pi,\pi)$, seen in structural experiments.[16] The lines going through the side sheets are simply displacements of the tight-binding fit by this Q vector. We find that all of the data is consistent with this picture, and it is not necessary, at least at the Fermi energy, to invoke the 2×2 modulation proposed by Aebi *et al.*[23] (we note that the samples of that group come from the same source as our own). In principle, more side sheets than two will occur, but presumably the intensity of these higher-order umklapps are reduced by matrix element effects.

Finally, we note that the area occupied by the observed Fermi surface is equivalent to a hole doping level of 17%, the same as that for optimal T_c in La-Sr-Cu-O. Using quoted values for the stoichiometries of the cations for our samples[14] ($Bi_{2.17}Sr_{1.77}Ca_{1.01}Cu_{2.05}O_{8+x}$) and the above hole count, we estimate an $x = 0.08$, which is consistent with a variety of published results.

III. SUPERCONDUCTING STATE

The method for extracting the gap has been discussed in detail in our earlier paper.[15] The Fermi momenta are obtained by finding the minimum separation of the quasiparticle peak from the chemical potential (operationally, when the leading edge of the energy distribution curve has the maximum slope). Experimentally the peak in the spectrum first approaches the chemical potential as k approaches k_F, then disperses away as k goes beyond k_F, with the intensity decreasing rapidly as expected from the momentum dependence of the coherence factors in BCS theory.

The spectral function is assumed to be that of BCS theory with a phenomenological linewidth to broaden the δ functions. Fortunately, this linewidth does not enter the fits at sufficiently low temperatures since the experimental spectra are resolution limited at 13 K where the gaps are measured (the gaps being determined by fitting the leading edge of the spectra). The spectral function is multiplied by the Fermi occupation factor and then integrated over momenta using the ±1 degree width of the analyzer window and convolved with the observed energy resolution function. The momentum integrations utilize the dispersion derived from the tight-binding fit. The background contribution affects the fits shown in Ref. 15 only at larger binding energies and thus does not influence the gap determination.

Besides the overall intensity, representing unknown matrix elements and normalization, this leaves only one adjustable parameter in the fit: the absolute value (magnitude) of the gap. The resulting gap values are plotted in Fig. 3. The basic point to note is that the data are consistent with nodes in the order parameter about 10° away from, and on both sides of, the (π,π) directions.

The data differ somewhat in the two quadrants, although it should be noted that the data in the two quadrants were taken on different samples since the analyzer does not have enough angular range to cover both quadrants in the geometry used. Nonetheless, repeated measurements on different samples yield consistent results for the momentum dependence of the gap, with the location of the nodes in the two quadrants being equivalent. We

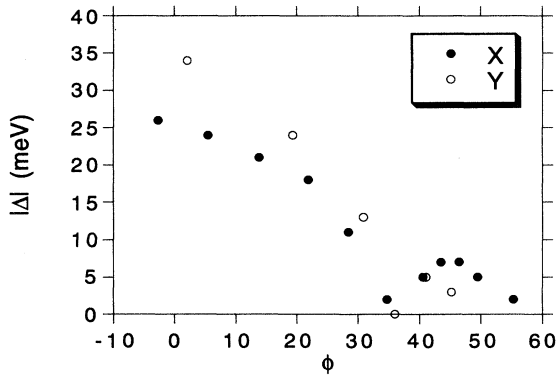

FIG. 3. Measured energy gap along the Fermi surface in the X and Y quadrants. The data for each quadrant were taken on a different sample. In this notation, 0° corresponds to the $\bar{M}-X,Y$ directions and 45° to the $\Gamma-X,Y$ directions, with the angle measured with respect to an origin at the X,Y points.

also note that in any particular quadrant, the measured gap has some sample dependence, as found in all ARPES work.

IV. d-WAVE AND RELATED MODELS

In this section we discuss the extent to which our results are compatible or incompatible with d-wave pairing. Some of the experimental evidence for and against d wave in Y-Ba-Cu-O was described in the Introduction. From a theoretical point of view it has been established[24] that if antiferromagnetic spin fluctuations mediate pairing then it must have $d_{x^2-y^2}$ symmetry. Experimentally the spin fluctuations in Bi-2212 have not been studied as intensively as in Y-Ba-Cu-O, nor are there any phase coherence experiments in Bi-2212. Recent NMR experiments[25] show a rapidly decreasing Knight shift below T_c, giving strong evidence for singlet pairing. The low-temperature Knight-shift and relaxation data suggest a gapless state which could arise from d-wave with impurity scattering, but gapless s-wave due to magnetic impurities cannot be ruled out.

Returning to the results of Fig. 3 we see that the data are inconsistent with a simple $d_{x^2-y^2}$ gap, since by definition such a gap must vanish along the (π,π) directions where $k_x = k_y$. Of course, Bi-2212 has a small orthorhombic distortion, which, even at T_c, can lead to mixing of $d_{x^2-y^2}$ with other symmetries. In Y-Ba-Cu-O, $d_{x^2-y^2}$ can mix with s wave, but in Bi-2212, it can mix only with g wave [A_{2g} representation of the form $(x^2-y^2)xy$], and thus would still have nodes along the diagonal directions. The difference occurs since in Y-Ba-Cu-O, the orthorhombic axes are along the CuO bond directions, whereas in Bi-2212, they are along the diagonal directions (and thus, reflection symmetry about the diagonal directions is preserved unlike in Y-Ba-Cu-O). Of course, s-d mixing can still occur in the nonlinear gap equations below T_c, but the above symmetry in Bi-2212 in a Ginzburg-Landau approach would imply two phase transitions instead of one.[26] We also note that an $s+d$ gap simply moves the node to one side or the other of the (π,π) direction; it cannot lead to nodes on both sides of (π,π), whereas an $s+id$ gap is nodeless.

Another alternative to consider is the dirty d-wave state which would produce a gapless region around (π,π). Even though we do not feel that the error bars on the gap estimation allow for this possibility, let us for the sake of argument assume that the small gaps in a $\pm 10^\circ$ region about the diagonal are all consistent with zero. Within the dirty d-wave theory, when such a large region of gaplessness is produced around (π,π) the large gap (near the $\bar{M}$ point here) would also be suppressed. Given that this gap is experimentally found to be quite sizable is further evidence against such an interpretation, although we caution that the degree of suppression is dependent on whether one assumes Born or unitary scattering. A more definitive test of dirty d-wave would be to conduct ARPES experiments as a function of disorder and compare to theoretical predictions.[27]

Superlattice effects

Next we comment on a possible interplay between a d-wave order parameter and the superlattice modulation in the X quadrant. These considerations were motivated by the fact that observed nodes in the X quadrant are located at the same points where the main Fermi surface sheet and the umklapped side sheets are predicted to cross. It should be noted at the outset that to the extent the location of the nodes in the X and Y quadrants are identical (within experimental resolution), the superlattice cannot be argued to have anything to do with nodes. Nevertheless, if one were to focus only on the X quadrant data, the coincidence noted above would require an explanation.

At this time no firm evidence exists in the data for superlattice effects in the X quadrant, primarily because the side sheets are not predicted to be well separated as they are in the Y quadrant. Because of this we do not know yet whether the superlattice modulation which exists on the BiO layers influences the CuO electronic structure causing a splitting of the sheets at the crossing points. It is possible that the BiO layer primarily acts as a diffraction grating for the outgoing photoelectrons (which would be sufficient to explain the effects seen in the Y quadrant). Nevertheless, since it will turn out that only a small superlattice potential on the CuO planes would give the effect described below, it cannot be *a priori* excluded.

At the crossing points, then, one has two bands and thus a 4×4 secular matrix to diagonalize (instead of the simple 2×2 secular matrix in BCS theory). Schematically this is given by

$$\begin{pmatrix} \epsilon & V & 0 & \Delta \\ V & \epsilon' & s\Delta & 0 \\ 0 & s\Delta & -\epsilon' & -V \\ \Delta & 0 & -V & -\epsilon \end{pmatrix} \tag{1}$$

and its eigenvalues determine the quasiparticle energies in the superconducting state. Here ϵ and ϵ' are the energies of the two bands measured from the chemical potential, V is the matrix element of the superlattice potential mixing the two bands, and Δ is the order parameter. The significance of the parameter $s = \pm 1$ will become clear below. It is instructive to focus on the analytically solvable case $\epsilon = \epsilon'$ which corresponds to a locus in $\mathbf{k}$ space where contours of constant energy of the two bands intersect.

First consider a gap function (e.g., an anisotropic s-wave gap) which is even with respect to reflections about the (π,π) direction. This corresponds to $s = +1$, since the gap is the same for the two sheets at the crossing point. The eigenvalues (for $\epsilon = \epsilon'$) are $E = \sqrt{(\epsilon \pm V)^2 + \Delta^2}$. Thus the superlattice potential just acts to "shift" the normal-state band structure but does not affect the nodes.

For the case of a $d_{x^2-y^2}$ gap, though, the gaps for the two sheets have *opposite* signs at the crossing points, which corresponds to $s = -1$. In this case, the quasiparticle energies are $E = \sqrt{\epsilon^2 + \Delta^2} \pm V$. This is qualitatively

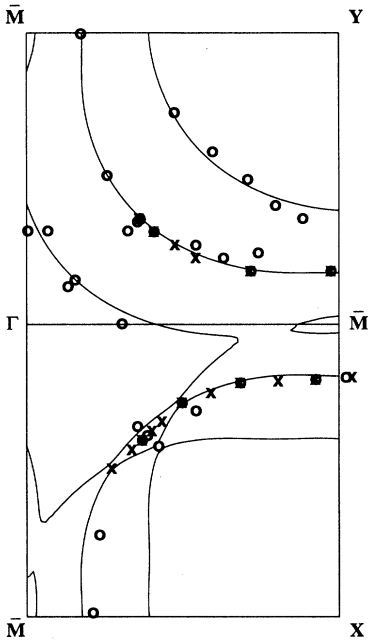

FIG. 4. Fermi surface determined by the tight-binding fit with an additional superlattice potential of 10 meV. Data points as in Fig. 1.

different from the previous case since the superlattice potential can now affect the locations of the nodes: if V exceeds Δ, a node in E must occur for some value of ϵ where there was none previously.

To study the second case in more detail we solve the 6×6 secular equation describing the main band and the two umklapped side bands using for each band the appropriate tight-binding energy dispersion in the X quadrant discussed above. In Fig. 4, we show a plot of the resulting Fermi surface assuming a superlattice potential of 10 meV (this potential is assumed to be the same for all off-diagonal terms; we note that the potential term connecting the two side bands to each other is in general different from that connecting the main sheet to the side sheets). In Fig. 5, we plot the resulting excitation gap (minimum of E) on the middle of the three sheets, assuming a $\cos(k_x) - \cos(k_y)$ order parameter. We note the dip in the excitation gap near the observed nodes. The finite gap along the $\Gamma - X$ direction occurs since the middle sheet corresponds to one of the side sheets in this case (the sheet nearest the Γ point along this direction corresponds to the main sheet and has a node; its gap is also shown in Fig. 5). Although Fig. 5 has remarkable similarities to Fig. 3, the main problem for such a model is that it predicts pure d-wave behavior for the excitation gap in the Y quadrant with a single node along $\Gamma - Y$, in contrast to experiment. As noted above, although the unusual anisotropy of the gap is more obvious in the X quadrant, one still sees qualitatively similar behavior in the Y quadrant.

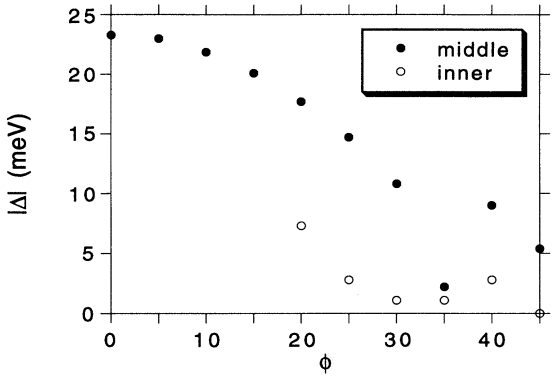

FIG. 5. Calculated excitation gap in the X quadrant assuming a $d_{x^2-y^2}$ order parameter with a coefficient of 12.5 meV and a superlattice potential of 10 meV on the middle of the three Fermi surface sheets shown in Fig. 4 (filled circles) and on the inner sheet nearest Γ (open circles).

Pairing within a bilayer

The final d-wave related scenario to consider is the interlayer pairing model of Ubbens and Lee.[28] In this model, it is assumed that the two CuO bands coming from the bilayer are degenerate (which is certainly consistent with our data) and that the pairing within a layer has $d_{x^2-y^2}$ symmetry while that between the two layers has an anisotropic s-wave symmetry. Again, one has a 4×4 secular matrix to diagonalize for the quasiparticle eigenvalues and the result is two excitation gaps of the form $d \pm s$. One of these gaps has a node on one side of the diagonal direction, the other on the other side. In Fig. 6, we show a fit of this theory to the data in the X quadrant assuming the s-wave component to be isotropic (which is probably a reasonable approximation

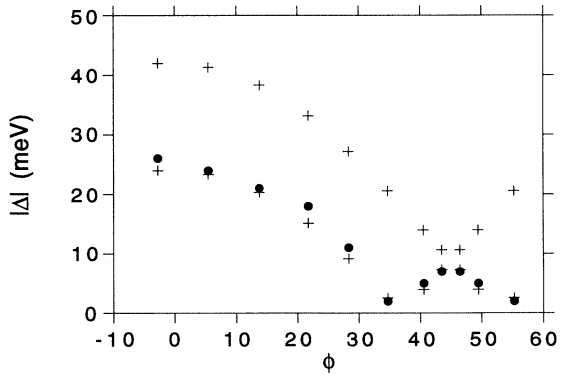

FIG. 6. Fit of the experimental data in the X quadrant to the smaller of the two gaps of the Ubbens and Lee model. Filled circles are the data and pluses (+) the two gaps of this model.

on the Fermi surface). The smaller of the two gaps fits the data quite well, however, there is no clear signature in the data of the larger of the two gaps at any point on the Fermi surface.

More specifically, all the spectra can be fit very well assuming one gap.[15] Two gap fits are possible, of course, given the finite resolution, but our fits to the spectrum at the maximum gap value (where the quasiparticle peaks are the sharpest) indicates that the largest splitting between the two gaps that can be accommodated by the data is about 10 meV. This should be contrasted with the 18 meV splitting implied by the fit. So we would conclude at this stage that the model of Ubbens and Lee is not inconsistent with the data, but that, so far, our data show no evidence for a second gap.

V. ANISOTROPIC s-WAVE MODELS

We now turn to a discussion of anisotropic s-wave pairing, by which we mean an order parameter which has the full symmetry of the lattice. While simple s-wave pairing corresponds to a gap function independent of $\mathbf{k}$, i.e., $\Delta(\mathbf{k}) = \Delta_0$, more general s-wave gap functions have the $\mathbf{k}$ dependence of the tight-binding functions listed in Table I. [We will not discuss functions, such as $|\cos(k_x) - \cos(k_y)|$, which have a singular $\mathbf{k}$ dependence at the node]. Examples of anisotropic s-wave pairing are the "extended s-wave" pairing, denoted by s^*

$$\Delta(\mathbf{k}) = \Delta_0[\cos(k_x) + \cos(k_y)] \tag{2}$$

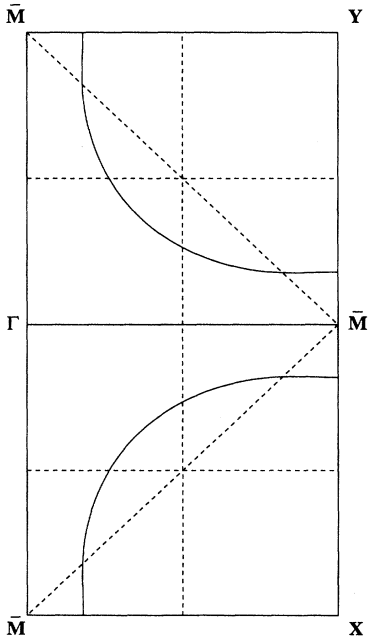

FIG. 7. Plots of the nodes of the s^* and s_{xy} functions in the Brillouin zone (dashed lines). The former run diagonally, the latter horizontally and vertically. The solid line marks the Fermi surface.

and s_{xy} pairing

$$\Delta(\mathbf{k}) = \Delta_0 \cos(k_x) \cos(k_y), \tag{3}$$

corresponding to the first two nontrivial entries in Table I, respectively. Note that for the purposes of this discussion we shall treat Bi-2212 as being tetragonal ignoring the effects of the superlattice. Figure 3 is clearly consistent with this type of order parameter in that the measured gap (a) appears to have an extremum along the diagonal directions which would require an order parameter which is even under reflection symmetry about this direction and (b) has nodes on both sides of the diagonal directions which is also allowed for this symmetry.

One of the early microscopic examples of anisotropic s-wave pairing was the s^* solution obtained by Littlewood, Varma, and Abrahams,[29] in the context of charge fluctuation mediated pairing in a three-band model. Depending on the precise shape of the Fermi surface an s^* gap has either no nodes (i.e., fully gapped) or two nodes per quadrant.[30] A more general phenomenological analysis was presented by Chen and Tremblay[31] who also discussed, among other things, the nodal structure of the s_{xy} state which will be shown to be relevant to the ARPES data.

Before discussing microscopic models, we first describe phenomenological fits to the ARPES gap data assuming a sign change in the gap function at the node observed in the experiment (so that the gap function is smooth at the node). In Fig. 7, we plot the location of the nodes of the s^* and s_{xy} gap in the Brillouin zone. We note that the nodes of the s_{xy} gap function are very close to the experimentally observed nodes in the excitation spectrum, whereas those of the s^* gap function are significantly further from the diagonal direction compared with the data. This can be seen more clearly in Fig. 8 where we plot these two functions over the observed Fermi surface. In fact, we find, quite surprisingly, that a pure s_{xy} gap fits the data very well in the X quadrant as shown in Fig. 9. A least-squares fit of the form $s^* + s_{xy}$ gives only a 2% admixture of s^* and one of the form $s + s_{xy}$ gives only a 0.2% admixture of the constant (s) term. Alternatively an $s + s^*$ gap can also fit the location of the nodes, but at

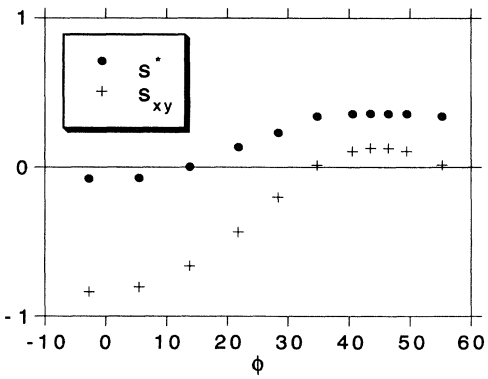

FIG. 8. Plots of the s^* and s_{xy} anisotropic s-wave functions along the Fermi surface in the X quadrant of the zone.

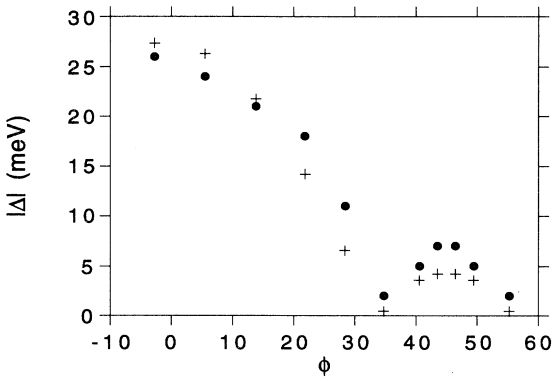

FIG. 9. Fit of the s_{xy} anisotropic s-wave gap to the data in the X quadrant. Filled circles are the data and pluses (+) the fit.

the expense of having too small a gap along the diagonal directions (this fit has the two terms comparable in size but with opposite sign).

Within a simple, single band BCS framework, given an effective electron-electron interaction $-V_{\mathbf{k},\mathbf{k}'}$, the gap function at a temperature T is determined by solving the self-consistent equation

$$\Delta(\mathbf{k}) = \sum_{\mathbf{k}'} V_{\mathbf{k},\mathbf{k}'} \frac{\Delta(\mathbf{k}')}{2E(\mathbf{k}')} \tanh\left[\frac{E(\mathbf{k}')}{2T}\right], \tag{4}$$

where $E(\mathbf{k}) = \sqrt{\epsilon^2(\mathbf{k}) + \Delta^2(\mathbf{k})}$. Here we will "invert" this procedure and infer some features of $V_{\mathbf{k},\mathbf{k}'}$ which would be consistent with the observed $\Delta(\mathbf{k})$. The simplest potentials which give rise to s, s^*, and s_{xy} pairing are attractive on-site, on the near-neighbor (NN) site, and on the next-near-neighbor (NNN) site, respectively.

The fact that a constant (s) term is not needed in the fit is significant in that it suggests that the large Coulomb repulsion on the Cu site is substantially renormalized in the pairing interaction between quasiparticles. We note that although the gap functions discussed above, other than the simple s state, satisfy the condition $\sum_{\mathbf{k}} \Delta(\mathbf{k}) = 0$, it is not this condition which must be satisfied to eliminate the effect of an on-site repulsion in the gap equations. Rather, it is the condition $\sum_{\mathbf{k}} \Delta(\mathbf{k})/2E(\mathbf{k}) \tanh[E(\mathbf{k})/2T] = 0$ which needs to be satisfied. Clearly, a pure s_{xy} function violates this condition which implies such a repulsive term in the gap equations must be small.[32]

The dominance of the NNN attraction in the singlet channel suggested by the s_{xy} pairing is also very interesting. To avoid any confusion, we emphasize that NNN means the NNN Cu site, and not the pairing of holes on neighboring oxygen sites. [The s_{xy} order parameter $\cos(k_x)\cos(k_y)$ Fourier transformed to real space has peaks in the relative coordinate near the $(\pm 1, \pm 1)$ primitive lattice vectors.] In most theories proposed to date, NNN pairing terms are weak and would play a minor role; in fact, we know of no theory where such terms determine the symmetry of the gap.

We now turn to microscopic models. The charge-transfer model of Varma and co-workers with s^* pairing was already mentioned earlier. The valence fluctuation model of Brandow[33] also gives rise to anisotropic s-wave pairing where the existence and location of nodes depends on the details of the input parameters and on the Fermi surface.

We finally discuss two other theories: the interlayer tunneling model of Chakravarty *et al.*[34] and the recent theory of Abrikosov[35,36] based on a weakly screened electron-phonon interaction in the presence of extended saddle-point singularities. While the physics underlying the two theories is completely different they share two characteristics: first, the dominant part of the interactions are "local in $\mathbf{k}$ space" (for entirely different reasons), and second, both theories have the ability of having different order-parameter symmetries in different materials with comparable T_c unlike in simple BCS models.

In Abrikosov's theory the poor screening of the electron-phonon interaction causes a sharp peak in the forward scattering direction (small momentum transfers). Further the local density of states is very large near the extended saddle-point singularity or flat band, around the $\bar{M}$ point in Bi-2212, and small away from it. The solution of the gap equation thus yields a highly anisotropic gap function which is large near $\bar{M}$ point and small away from it. An additional short-range Coulomb repulsion is required to produce nodes as pointed out recently by Abrikosov.[36] This adds an overall negative constant to the order parameter, thus causing the small order parameter along the diagonal direction to become negative, with nodes on two sides of the diagonal in a tetragonal material like Bi-2212. However in an orthorhombic material like YBCO, which in this theory is modeled as having an extended saddle point only along one direction, Abrikosov finds an $s + d$ gap with a sign change going from the a to the b axis.

The model of Chakravarty *et al.* is based on ideas of Anderson[20] that the elementary excitations, the holons and spinons, are confined within a plane, and thus the coherent transport of single electrons from one plane to another is not possible (this is certainly consistent with our observation of only one CuO band). The dominant interaction is the tunneling of Cooper pairs between layers which lowers the kinetic energy dramatically and thus acts to drive the superconducting transition. This pair tunneling term, which is assumed to be completely local in momentum space, leads to the high-T_c but does not constrain the symmetry of the order parameter. The in-plane BCS interaction, which is a weak additive term, is as usual nonlocal in momentum variables and thus determines the symmetry of the gap, with the momentum dependence of this gap being modulated by the $\mathbf{k}$ dependence of the tunneling term $t_\perp(\mathbf{k})$. [In Bi-2212 electronic structure calculations suggest that $t_\perp(\mathbf{k})$ is large along the CuO bond direction and small along the diagonal direction.] In the model of Chakravarty *et al.*, the largest of the weak in-plane BCS terms could differ from one material to another, thus leading to the possibility mentioned in the beginning of this paper of different pairing symmetries for different cuprates.

VI. CONCLUSIONS

In conclusion, we have analyzed various theoretical models in light of our measured gap anisotropy in Bi-2212. We find that a simple d-wave model can be made consistent with the data in the X quadrant, but not in the Y quadrant, if the superlattice modulation is taken into account. We find that the only d-wave model consistent with the observed behavior in both quadrants is an interlayer pairing model[28] although we remark that so far, we have no evidence for the two-gap spectrum required by such a model. The simplest gap function which naturally explains the two nodes observed per quadrant is an s_{xy} order parameter of the form $\Delta_0 \cos(k_x) \cos(k_y)$. Within a one-band BCS framework such an order parameter is obtained from a next-near-neighbor (Cu-Cu) interaction. Several microscopic theories[29,33–36] which give rise to anisotropic s-wave pairing were discussed in this context.

ACKNOWLEDGMENTS

We would like to thank Alex Abrikosov, Phil Anderson, Baird Brandow, Sudip Chakravarty, Roland Fehrenbacher, Patrick Lee, and Chandra Varma for helpful discussions. This work was supported by the U. S. Department of Energy, Basic Energy Sciences, under Contract No. W-31-109-ENG-38.

[1] W. N. Hardy *et al.*, Phys. Rev. Lett. **70**, 3999 (1993).
[2] D. A. Wollman *et al.*, Phys. Rev. Lett. **71**, 2134 (1993) and **74**, 797 (1995); D. A. Brawner and H. R. Ott, Phys. Rev. B **50**, 6530 (1994); A. Mathai *et al.* (unpublished).
[3] C. C. Tsuei *et al.*, Phys. Rev. Lett. **73**, 539 (1994); J. R. Kirtley *et al.*, Nature (London) **373**, 225 (1995).
[4] A. G. Sun *et al.*, Phys. Rev. Lett. **72**, 2267 (1994).
[5] P. Chaudhari and S.-Y. Lin, Phys. Rev. Lett. **72**, 1084 (1994) and S.-Y. Lin *et al.* (unpublished).
[6] D. H. Wu *et al.*, Phys. Rev. Lett. **70**, 85 (1993).
[7] Q. Huang *et al.*, Nature (London) **347**, 369 (1990).
[8] J. Chen *et al.*, Phys. Rev. B **49**, 3683 (1994).
[9] Z.-X. Shen *et al.*, Phys. Rev. Lett. **70**, 1553 (1993).
[10] C. G. Olson *et al.*, Solid State Commun. **76**, 411 (1990).
[11] H. Ding *et al.*, Phys. Rev. B **50**, 1333 (1994).
[12] R. J. Kelley *et al.*, Phys. Rev. B **50**, 590 (1994).
[13] A. Bansil *et al.*, J. Phys. Chem. Solids **54**, 1185 (1993).
[14] T. Mochiku and K. Kadowaki (unpublished).
[15] H. Ding *et al.*, Phys. Rev. Lett. **74**, 2784 (1995).
[16] R. L. Withers *et al.*, J. Phys. C **21**, 6067 (1988).
[17] S. Massidda, J. Yu, and A. J. Freeman, Physica C **152**, 251 (1988); H. Krakauer and W. E. Pickett, Phys. Rev. Lett. **60**, 1665 (1988).
[18] C. G. Olson *et al.*, Phys. Rev. B **42**, 381 (1990).
[19] D. S. Dessau *et al.*, Phys. Rev. Lett. **71**, 2781 (1993).
[20] P. W. Anderson, Science **256**, 1526 (1992); *A Career in Theoretical Physics* (World Scientific, Singapore, 1994), p. 638.
[21] K. Gofron *et al.*, J. Phys. Chem. Solids **54**, 1193 (1993); Phys. Rev. Lett. **73**, 3302 (1994).
[22] O. K. Andersen, O. Jepsen, A. I. Liechtenstein, and I. I. Mazin, Phys. Rev. B **49**, 4145 (1994).
[23] P. Aebi *et al.*, Phys. Rev. Lett **72**, 2757 (1994). Recently, we have also seen the "shadow" band in the Y quadrant away from the Fermi energy. Whether this is due to magnetic correlations or to the orthorhombic unit cell is an open question.
[24] N. E. Bickers, D. J. Scalapino, and R. T. Scaletar, Int. J. Mod. Phys. B **1**, 687 (1987); T. Moriya, Y. Takahashi, and K. Ueda, J. Phys. Soc. Jpn. **59**, 2905 (1990); P. Monthoux, A. V. Balatsky, and D. Pines, Phys. Rev. Lett. **67**, 3448 (1991).
[25] M. Takigawa and D. B. Mitzi, Phys. Rev. Lett **73**, 1287 (1994).
[26] P. Kumar and P. Wolfle, Phys. Rev. Lett. **59**, 1954 (1987); Q. P. Li, B. E. C. Koltenbah, and R. Joynt, Phys. Rev. B **48**, 437 (1993).
[27] R. Fehrenbacher and M. R. Norman, Phys. Rev. B **50**, 3495 (1994).
[28] M. U. Ubbens and P. A. Lee, Phys. Rev. B **50**, 438 (1994).
[29] P. B. Littlewood, C. M. Varma, and E. Abrahams, Phys. Rev. Lett. **63**, 2602 (1989); P. B. Littlewood, Phys. Rev. B **42**, 10 075 (1990).
[30] A. J. Fedro and D. D. Koelling, Phys. Rev. B **47**, 14 342 (1993).
[31] L. Chen and A.-M. S. Tremblay, J. Phys. Chem. Solids **54**, 1381 (1993).
[32] R. Fehrenbacher and M. R. Norman, Phys. Rev. Lett. **74**, 3884 (1995).
[33] B. H. Brandow, Int. J. Mod Phys. B **8**, 2667 (1994).
[34] S. Chakravarty, A. Subdo, P. W. Anderson, and S. Strong, Science **261**, 337 (1993).
[35] A. A. Abrikosov, Physica C **222**, 191 (1994).
[36] A. A. Abrikosov, Phys. Rev. B (to be published); Physica C **244**, 243 (1995).